Pivotal role of mixed-layer depth in Tropical Atlantic Multidecadal Variability

ADVANCING EARTH AND SPACE SCIENCES

Geophysical Research Letters

RESEARCH LETTER
10.1029/2024GL110057

Pivotal Role of Mixed-Layer Depth in Tropical Atlantic Multidecadal Variability

Balaji Senapati[1], Christopher H. O'Reilly[1], and Jon Robson[2]

[1]Department of Meteorology, University of Reading, Reading, UK, [2]Department of Meteorology, National Centre for Atmospheric Science, University of Reading, Reading, UK

Key Points:

- Tropical Atlantic Multidecadal Variability (AMV) is driven by wind-mixed-layer-sea surface temperature (SST) feedback in extratropical SST-restoring experiments
- Weakening of trade winds in summer induces a shallower mixed-layer, reducing ocean heat capacity and generating positive tropical AMV
- Changes in surface heat-fluxes or associated mechanisms are not responsible for tropical AMV in these experiments

Supporting Information:

Supporting Information may be found in the online version of this article.

Correspondence to:

B. Senapati,
b.senapati@reading.ac.uk

Citation:

Senapati, B., O'Reilly, C. H., & Robson, J. (2024). Pivotal role of mixed-layer depth in tropical Atlantic multidecadal variability. *Geophysical Research Letters*, *51*, e2024GL110057. https://doi.org/10.1029/2024GL110057

Received 2 MAY 2024
Accepted 29 JUL 2024

Author Contributions:

Conceptualization: Balaji Senapati, Christopher H. O'Reilly
Formal analysis: Balaji Senapati
Funding acquisition: Christopher H. O'Reilly
Investigation: Balaji Senapati, Christopher H. O'Reilly, Jon Robson
Methodology: Balaji Senapati, Christopher H. O'Reilly
Resources: Christopher H. O'Reilly
Supervision: Christopher H. O'Reilly, Jon Robson
Visualization: Balaji Senapati
Writing – original draft: Balaji Senapati
Writing – review & editing: Christopher H. O'Reilly, Jon Robson

Abstract The tropical arm of Atlantic Multidecadal Variability (AMV) influences climate worldwide, yet the mechanisms generating it remain unclear. Here, we examine experiments with sea surface temperature (SST)-restoring in the extratropical North Atlantic in multiple models and use mixed-layer heat budgets to elucidate the important mechanisms. Our results demonstrate that the tropical AMV is driven by wind-mixed-layer-SST feedback. The evolution has two phases with tropical AMV SST anomalies growing from April to October and decaying from November to March. The amplitude of the growth phase surpasses that of the decay phase, resulting in overall tropical Atlantic warming during positive AMV phases. During summer, positive SST anomalies in the extratropics weaken the trade winds, resulting in a shallower mixed-layer with reduced heat capacity. Subsequent absorption of climatological shortwave radiation in this shallower mixed-layer then causes SSTs to warm, generating the tropical AMV. Importantly, anomalous surface heat-fluxes make modest contributions to tropical AMV in these experiments.

Plain Language Summary The North Atlantic sea surface temperature (SST) has fluctuated significantly over periods of decades to multiple decades, a phenomenon known as the Atlantic Multidecadal Variability (AMV). It influences climate worldwide; however, questions remain about how it evolves. This study highlights the vital role of upper ocean processes, particularly the depth of oceanic mixed-layer, in generating the tropical part of the AMV. Here, we analyzed SST-restoring climate model experiments in which a surface temperature anomaly is added over the extratropical North Atlantic Ocean. The evolution features a summer growth phase and a winter decay phase, with stronger growth leading to overall warming during positive phases of the tropical AMV. In summer, prevailing trade winds weaken and induce a shallower depth of oceanic mixed-layer. This leads to the absorption of solar energy in a reduced volume of ocean water, resulting in the warming of SST and the development of a positive phase of tropical AMV. Interestingly, changes in heat-fluxes over the ocean surface and related mechanisms make little contribution to the development of tropical AMV in these experiments. These results emphasize the importance of accurate upper-ocean processes for the simulation of AMV in coupled climate models.

1. Introduction

The North Atlantic sea surface temperature (SST) undergoes distinct multidecadal fluctuations, which reflect a mode of climate variability commonly referred to as Atlantic Multidecadal Variability (AMV) (Delworth & Mann, 2000; Kerr, 2000). The AMV significantly influences global climate, influencing North American and European climates, as well as impacting North African climate, Atlantic hurricane activity, and global monsoon (Goldenberg et al., 2001; Knight et al., 2006; Martin et al., 2014; Monerie et al., 2019; O'Reilly et al., 2017; Ruprich-Robert et al., 2018; Sutton & Hodson, 2007; Ting et al., 2011; R. Zhang & Delworth, 2006). In fact, the tropical sector of the AMV appears to drive many global-scale impacts (Dong et al., 2006; Kucharski et al., 2016; McGregor et al., 2014; Monerie et al., 2019; Ruprich-Robert et al., 2017; Sutton & Hodson, 2005). Despite its importance, the tropical AMV signal is often underestimated in coupled models (Kavvada et al., 2013; Martin et al., 2014; L. Zhang & Wang, 2013), and the mechanisms underlying its development remain uncertain.

Recent research highlights the crucial role of interactive air-sea feedbacks, including wind-evaporation-SST, cloud, and dust feedbacks, in transmitting the Atlantic Meridional Overturning Circulation-induced AMV SST signal from the subpolar to the tropical North Atlantic along the so-called "horseshoe" pathway (Bellomo et al., 2016; Brown et al., 2016; Drews & Greatbatch, 2017; Hodson et al., 2014; Kavvada et al., 2013; Wang et al., 2012; Yuan et al., 2016; R. Zhang et al., 2019). These studies have suggested that warm subpolar SST anomalies induce cyclonic atmospheric circulation, weakening trade winds. The weakened trade winds result in reduced evaporation, Saharan dust emission and transport, and low cloud cover over the tropical North Atlantic. Some studies suggested that the wind-evaporation-SST feedback contributes to warm tropical AMV through reduced evaporation (Chang et al., 1997; Smirnov & Vimont, 2012), while others suggest that decreased dust and cloud cover allow more solar radiation to warm the tropical AMV, referred to as dust and cloud feedbacks (Bellomo et al., 2016; Brown et al., 2016; Yuan et al., 2016). These feedbacks are suggested to amplify the tropical AMV signal by modulating the radiative/turbulent heat-fluxes over the region (Bellomo et al., 2016; Brown et al., 2016; Wang et al., 2012; Yuan et al., 2016).

However, these observational and modeling analyses have limitations. Bellomo et al. (2016) raised concerns about the proposed positive cloud and dust feedbacks by Brown et al. (2016) and Yuan et al. (2016), noting issues such as short observational record and not removing trends from the cloud cover analysis. They highlighted that the power of tropical Atlantic SST variability remained unchanged in a modeling experiment without cloud feedback (Brown et al., 2016). Considering this, Bellomo et al. (2016) used a long observational record, removed trends, and estimated that cloud feedbacks contribute only 10%–17% of observed tropical Atlantic SST anomalies associated with the AMV. These findings raise an important question: What is the dominant mechanism missing that plays a role in the development of tropical AMV?

In their study, Bellomo et al. (2016) used an AGCM coupled to a slab ocean model with fixed mixed-layer depth (MLD), to quantify the contribution of cloud feedback for the analysis; but this approach potentially misses key processes associated with mixed-layer depth changes and associated feedbacks. Indeed, it is known that changes in mixed-layer depth can have important implications for SST anomalies (see Morioka et al. (2011); Morioka et al. (2012); Senapati et al. (2024)). Recently, Yamamoto et al. (2020) emphasized the significance of multi-decadal variations in MLD for the emergence of the AMV SST signal over the subpolar region, driven by the multidecadal North Atlantic Oscillation. In the subpolar Atlantic, a deeper mixed-layer depth enhances the ocean's heat capacity, making it less sensitive to surface cooling from heat-fluxes and causing relative warming. The variation in MLD is caused by the anomalous salinity transport by the Gulf Stream, which is modulated by the multidecadal North Atlantic Oscillation. Additionally, Liu et al. (2023) highlighted the role of oceanic processes, including seasonal MLD variation and entrainment, using a hierarchy of stochastic models in the multidecadal variability of extratropical Atlantic SST.

However, to date, the role of mixed-layer depth variability and feedbacks in the tropical North Atlantic and their role in governing the development of AMV has received little attention, leaving us far from understanding the dominant mechanisms at play in tropical AMV. Indeed, a deeper insight into these mechanisms, particularly by way of their seasonal evolution, is essential not only for advancing our comprehension of AMV but also for enhancing the accuracy of coupled models in simulating AMV more effectively.

In this study, we aim to fill this gap by analyzing the emergence of tropical Atlantic SST anomalies associated with the AMV in idealized multi-model SST-restoring experiments. We specifically analyze the air-sea interaction processes seasonally, quantifying the contribution from upper ocean processes and other feedbacks related to surface fluxes. Our findings indicate that the upper ocean mixed-layer dynamics are found to play a crucial role in governing the evolution of the tropical AMV, with significant implications for climate models aiming to simulate the tropical AMV and its associated global impacts successfully.

2. Data and Methodology

2.1. SST-Restoring Experiments

We analyze the monthly-mean output from three climate models that have each run the *dcppC-amv-ExTrop* experiments in the Coupled Model Intercomparison Project 6 (CMIP6) archive (Boer et al., 2016): CNRM-CM6-1 (hereafter CNRM), IPSL-CM6A-LR (hereafter IPSL), and HadGEM3-GC31-MM (hereafter HadGEM). The experiments restore SSTs in the extratropical North Atlantic region (30–60°N, 80–0°W; green boxes in Figure 1) and more effectively capture air-sea interaction processes in the region (O'Reilly et al., 2023). Specifically, the model's SST, within the ocean model component, is nudged toward either a positive (AMV+) or negative (AMV−) observed AMV anomaly pattern in the extratropical North Atlantic region. The details of the SST-restoring experiments are outlined in "three Technical Notes dealing with Component C experiments" available at https://www.wcrp-climate.org/experimental-protocol. There are 40, 25, and 25 ensemble members in

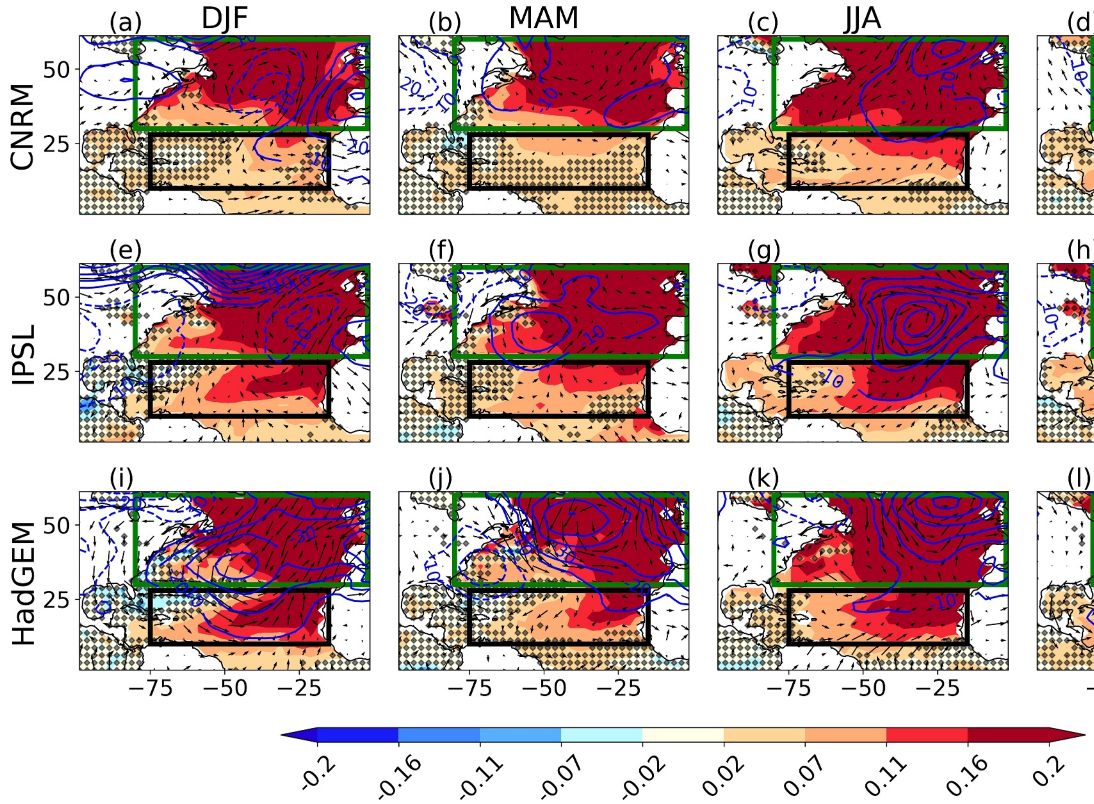

Figure 1. Seasonal SST anomalies (shading; in °C), sea level pressure anomalies (contours; in Pascal; solid contour represents the low pressure) and anomalous 925 hPa wind (vector; in ms^{-1}) are presented row-wise for three climate models. The first to the fourth columns correspond to December-January-February (DJF), March-May (MAM), June-August (JJA), and September-November (SON), respectively. A 3-month running mean is applied to smooth the time series. Stippling indicates where the SST anomalies are within the 90% confidence intervals (estimated using a Student's *t*-test). The green rectangular box shows the region where SST anomalies are nudged toward the observed AMV anomaly pattern. The black box is the tropical Atlantic region used for further analysis.

each of the AMV+ and AMV− pacemaker experiments for the CNRM, IPSL, and HadGEM coupled models, respectively, and all simulations span 10-years. Here, we define the AMV-related anomaly as the difference between the ensemble mean of AMV+ and AMV− experiments, using the entire 10-years data set for each member.

2.2. SST Budget

The evolution of the tropical sector (10–30°N, 75–15°W; black box in Figure 1) of AMV is assessed by performing SST budget analysis over the region. The evolution of SST anomalies can be expressed as:

$$\underbrace{\frac{\partial SST}{\partial t}}_{SST\ tendency} = \frac{\partial T_m}{\partial t} = \underbrace{\frac{Q_{net} - q_{(-H)}}{\rho c_p H}}_{Flux\ term} + \underbrace{\frac{Q_{ek}}{\rho c_p H}}_{Ekman\ term} + Residual, \tag{1}$$

where T_m is the mixed-layer temperature (equivalent to SST; Alexander and Scott (2008); Deser et al. (2010)), H is the mixed-layer depth, ρ is the density of seawater, and c_p is the specific heat capacity. The terms on the right-hand side represent the SST tendency driven by net surface heat-flux (first term) and Ekman heat transport (second term). The net surface heat-flux at the ocean surface (Q_{net}) comprises the net shortwave radiation (Q_{SW}), sensible heat-flux (Q_{SHF}), net longwave radiation (Q_{LW}), and latent heat-flux (Q_{LHF}). In this study, we use the convention that heat-flux is positive downwards, such that positive heat-flux warms the ocean. The $q_{(-H)}$ in the Q_{net} term is the downward radiative heat-flux at the bottom of the mixed-layer, computed following Paulson and Simpson (1977).

The second term in Equation 1, $Q_{ek}\left[=\frac{c_p}{f}\left(\tau_y\frac{\partial SST}{\partial x}-\tau_x\frac{\partial SST}{\partial y}\right)\right]$, is the heat-flux due to Ekman advection (Frankignoul, 1985). Here, f, τ_x, and τ_y represent the Coriolis parameter, zonal wind stress, and meridional wind stress, respectively.

The *Residual* term in Equation 1 also includes other oceanic contributions, such as horizontal and vertical advection terms. We do not explicitly analyze this term here because it is either small or opposite the SST tendency, implying that these do not have a leading order effect in driving the SST changes, as we will show in the results that follow.

The SST budget is analyzed separately for AMV+ and AMV− experiments, and then all analyses are presented as differences, referred to as anomalies.

To further explore the heat-flux contributions to the SST anomalies, we decompose the contribution of surface heat-fluxes in Equation 1 into two parts (following, e.g., Morioka et al., 2010; Senapati et al., 2024):

$$\underbrace{\delta\left(\frac{Q_{net}-q_{-H}}{\rho c_p H}\right)}_{\textit{Flux term}}\left[\equiv\delta\left(\frac{Q}{\rho c_p H}\right)\right]=\underbrace{\frac{\delta Q}{\rho c_p\overline{H}}}_{\substack{\textit{Due to}\\ \textit{flux}\\ \textit{anomaly}}}-\underbrace{\frac{\delta H\overline{Q}}{\rho c_p\overline{H}^2}}_{\substack{\textit{Due to}\\ \textit{MLD}\\ \textit{anomaly}}}+\textit{Residual.} \tag{2}$$

Overbar and $\delta()$ represent the climatology (mean of AMV+ and AMV−) and their differences, respectively. The first term on the r.h.s. contributes to the SST tendency due to surface heat-flux anomalies (δQ) acting on a climatological MLD $(\overline{H})$. Similarly, the second term is driven by MLD anomalies (δH) under climatological heating/cooling $(\overline{Q})$.

2.3. Monin-Obukhov Depth Calculation

The Monin-Obukhov depth (H_{MO}) in the upper ocean is a measure of the depth of the homogenous layer influenced by both turbulent mixing and buoyancy effects. It is used as a diagnostic for computing the drivers of MLD changes (Kraus & Turner, 1967; Qiu & Kelly, 1993). In summer, when the mixed-layer is in the shoaling phase, H_{MO} can be expressed as:

$$H_{MO}=\frac{m_0 u_*^3}{Q_*}+\frac{q_*}{Q_*}, \tag{3}$$

where, $Q_*\left[=\frac{\alpha g}{2\rho c_p}\left(Q_{\text{net}}-q_{(-H)}\right)\right]$ is the effective buoyancy forcing, the wind stirring represented by $m_0 u_*^3$, and $q_*\left[=\frac{\alpha g}{\rho c_p}\int_{-H_{MO}}^{0}q(z)dz\right]$ denotes the effective penetrative shortwave radiation. Here, m_0 (=0.5) is the coefficient of wind stirring (Davis et al., 1981), and u_* is the frictional velocity $\left[u_*=\sqrt{\frac{|\tau|}{\rho}}\right]$, where τ is wind stress. g (=9.8 ms^{-1}) represents the acceleration due to gravity, α (=0.00025°C^{-1}) denotes the coefficient of thermal expansion in water and $q(z)$ represents the downward solar insolation calculated following Paulson and Simpson (1977). The ratio of $m_0 u_*^3$ to Q_* signifies the H_{MO} due to the wind stirring term, and the ratio of q_* to Q_* represents H_{MO} due to buoyancy forcing.

3. Tropical AMV Evolution and Inconsistent Surface Heat-Flux Forcing

We start the analysis to understand the seasonal evolution of tropical AMV in the SST-restoring experiments (see methods). Figure 1 shows the seasonality of AMV anomalies in SST (shading), sea level pressure (contours) and 925 hPa wind (vectors) in the three different models. The evolution of tropical AMV is generally similar among the models, albeit with notable amplitude differences, particularly in the CNRM model. For example, the SST anomaly in the CNRM model is notably lower than in others during DJF (Figures 1a, 1e, and 1i). However, we are particularly interested in the evolution of the tropical AMV rather than the specific amplitude differences, so the similarities in the seasonality suggest there may be common mechanisms governing the evolution across the

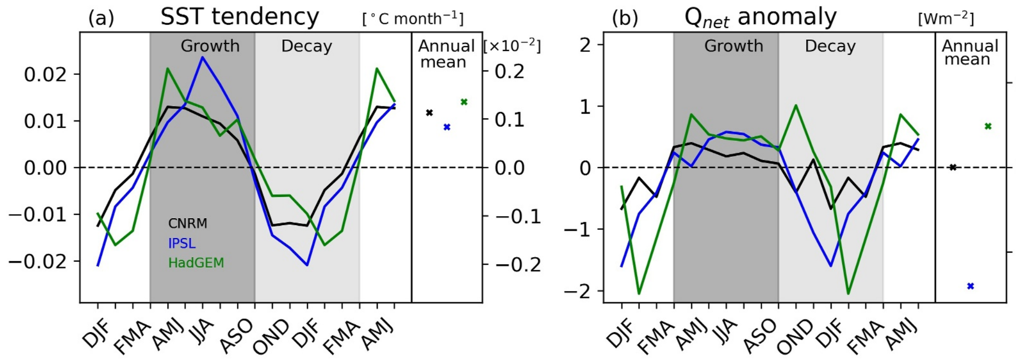

Figure 2. (a) Difference of seasonal SST tendency (in °C month $^{-1}$) in AMV+ and AMV− SST-restoring experiments and its mean (i.e., marked by asterisk; values in the secondary *y*-axis) over the tropical North Atlantic. The X-axis is extended up to 18 months to aid interpretation. Panel (b) similar to (a) but for net surface heat-flux anomaly (in W m^{-2}). Dark and light gray indicates the growth and decay phases. Black, blue, and green colors refer to CNRM, IPSL, and HadGEM models, respectively. A 3-month running mean is applied to smooth the time series. A positive value of flux indicates the warming of the ocean.

models. The tropical SST anomalies are positive throughout all seasons, peaking in the boreal autumn, September-November, and are at their minimum during the spring, March-May. The SST anomalies develop in a northeast-southwest direction, forming the familiar horseshoe pattern in September-November, and then gradually decay (Figure 1).

The seasonal evolution of SST anomaly typically aligns with low sea level pressure (solid contours) and associated wind anomaly patterns (Figure 1). From June to August, low pressure in the extratropical North Atlantic, particularly on its eastern side, extends into the tropical region and is associated with weakened trade winds. This pattern intensifies, reaching its peak in the autumn (September-November), before declining in winter. These circulation anomalies are consistent with those found in the SST-restoring experiments analyzed by Monerie et al. (2019) (i.e., their Figures 4e and 4f). Various mechanisms linking trade wind weakening to SST warming in the tropical Atlantic have been proposed (see Introduction), including wind-evaporation-SST, cloud, and dust feedbacks, which suggest that changes in surface heat-fluxes drive the changes in SST (Bellomo et al., 2016; Brown et al., 2016; Chang et al., 1997; Smirnov & Vimont, 2012; Wang et al., 2012; Yuan et al., 2016).

To analyze the role of surface heat-fluxes in governing the seasonal evolution of the SST anomaly associated with AMV, we first plot the seasonal SST tendency (Figure 2a) in the tropical Atlantic region (indicated by the black box in Figure 1). Figure S1 in Supporting Information S1 shows the SST tendency among ensemble members and the standard error around the ensemble mean. The positive SST tendency, indicating the growth phase of tropical AMV anomalies, extends from April to October, while the negative SST tendency, representing the decay phase of tropical AMV, occurs from November to March (Figure 2a). This means that the SST tendency in the tropical AMV (Figure 2a) is more positive than the climatological state (Figure S2b in Supporting Information S1) during the growth phase, causing more warming. During the decay phase, the SST tendency is more negative (Figure 2a) than the climatological state (Figure S2b in Supporting Information S1), leading to more cooling. Though there are differences in SST amplitudes across the models (Figure 1), the seasonal SST tendencies are broadly similar across models (Figure 2a). It is important to note that the seasonal cycle of SST anomalies is consistently positive, peaking in autumn and reaching a minimum in spring, which is consistent across all models (Figure 1). Further analysis reveals that the different SST anomalies that emerge within the first month/year of the simulations differ substantially across the models and are largely responsible for the amplitude differences (not shown). Nonetheless, the broad consistencies in the SST tendencies indicate that similar mechanisms may underlie the tropical SST evolution across the different models. Figure 2b shows the seasonal and annual Q_{net} anomaly over the tropical Atlantic. In the growth phase of tropical AMV (Figure 2a), a modest positive anomaly in Q_{net} is observed in all the models (Figure 2b). Conversely, during the decay phase of tropical AMV (Figure 2a), a negative Q_{net} anomaly is evident (Figure 2b). Thus, on initial inspection, these results seem to align with past studies, which implicated surface heat-flux anomalies for the development of the tropical AMV through changes in evaporation (Chang et al., 1997; Smirnov & Vimont, 2012; Yamamoto et al., 2020; R. Zhang et al., 2019), changes in cloud-cover (Bellomo et al., 2016; Brown et al., 2016; Yuan et al., 2016), or changes in dust (Wang et al., 2012; Yuan et al., 2016).

It is interesting to note, however, that the annual mean Q_{net} anomaly is inconsistent across the three models: CNRM with nearly zero, HadGEM with positive, and IPSL with a negative value (Figure 2b) - this is despite the annual mean SST tendencies being very similar across the models (i.e., Figure 2a; Table S1 in Supporting Information S1). In addition, the amplitudes of Q_{net} anomalies are all very small. Together, this raises questions about whether surface heat-flux anomalies really control SST anomalies in the tropical sector of the AMV. It is important to note that the amplitude of the SST tendency in the growth phase is greater than in the decay phase giving the overall positive annual-mean tendency in positive AMV (Figure 2a; Table S1 in Supporting Information S1). Hence, the tropical Atlantic warms overall during positive AMV phases (shading; Figure 1) because of processes controlling the seasonal evolution of SST. As a result, the SST anomaly remains positive throughout all seasons in the positive phase of AMV (solid lines in Figure S3 in Supporting Information S1). In the next section, we show that the Q_{net} anomalies alone are insufficient to account for the SST tendencies seen in the experiments.

4. Budget Analysis of the Tropical Atlantic SST

To quantify the processes influencing the growth and decay of SST, we conducted a SST budget analysis (i.e., Equation 1) over the tropical Atlantic region (black box in Figure 1). Figures 3a, 3b, and 3c show the SST budget terms (i.e., Equation 1) for the CNRM, IPSL, and HadGEM models, respectively. The growth and decay of the SST anomalies (solid black line) over the tropical Atlantic are both dominated by the Q_{net} term (blue line). The SST anomaly term increases/grows from April to October in phase with Q_{net} until the Q_{net} turns negative, leading to a subsequent decrease/decay in the SST anomaly. In comparison, the Ekman term (green line) contributes weakly to the growth phase, but it is negligible for the decay of the tropical AMV. The residual term (pink line) is either negligible (in the CNRM and IPSL models) or exhibits an opposite trend (in the HadGEM model) to the SST tendency; the latter potentially indicating a prominent role of ocean dynamics in damping the SST tendencies during growth/decay (e.g., through changes in horizontal or vertical advection). Nonetheless, it is clear that the residual term is not actively controlling the timing of the growth/decay phases in any of the models. To better understand the role of the surface heat-flux in the SST budget, we split the Q_{net} term into four components (i.e., Q_{SW}, Q_{LW}, Q_{LHF}, and Q_{SHF}), as illustrated in Figures 3d–3f. We find that the anomalous Q_{SW} term (black line) consistently warms the tropical Atlantic, peaking during the growth phase. In contrast, the anomalous Q_{LHF} and Q_{LW} terms (red and green lines) contribute to cooling SSTs. Contributions from the Q_{SHF} term (cyan line) are negligible. During the growth phase, the Q_{SW} term dominates in warming the SST anomaly over the tropical Atlantic despite damping from other flux terms. Similarly, the Q_{LHF} term dominates the decay phase in tropical AMV. Overall, the budget analysis demonstrates that the seasonal growth of tropical AMV from April to October is dominated by the Q_{SW} term, while its decay from November to March is mainly controlled by the Q_{LHF} term.

Whilst the budget analysis yields relatively clear results, the anomalies in the direct surface heat-flux - shown in Figures 3g–3i - seem potentially inconsistent with the budget analysis. The Q_{net} anomaly (blue line) is primarily influenced by the anomalous Q_{LHF} (red line) (Figures 3g–3i). Interestingly, the negative Q_{SW} anomaly might be expected to induce cooling of SST in the CNRM and IPSL models during the growth phase. In contrast, positive Q_{SW} acts to warm the ocean in the early growth phase and negative Q_{SW} acts to cool the ocean in the late growth phase in the HadGEM model. The evolution of the Q_{SW} anomaly is in contrast to previous studies that have suggested changes in shortwave fluxes, in response to changes in cloud-cover or dust, are responsible for the tropical SST anomalies associated with AMV (Bellomo et al., 2016; Brown et al., 2016; Yuan et al., 2016). The conflicting characteristics of the SST budget terms (i.e., Figures 3d–3f) and the direct heat-flux anomalies (i.e., Figures 3g–3i) suggest that changes in the mixed-layer depth, which appears in the denominator of the budget terms, may play an important role in governing the seasonal evolution of the SST tendency. We will analyze the role of mixed-layer changes in the next section.

5. Role of Oceanic Mixed-Layer in Tropical AMV

To examine the influence of mixed-layer depth changes in the seasonal evolution of the SST tendency, we now decompose the surface heat-flux budget terms into two components, one that depends on surface heat-flux

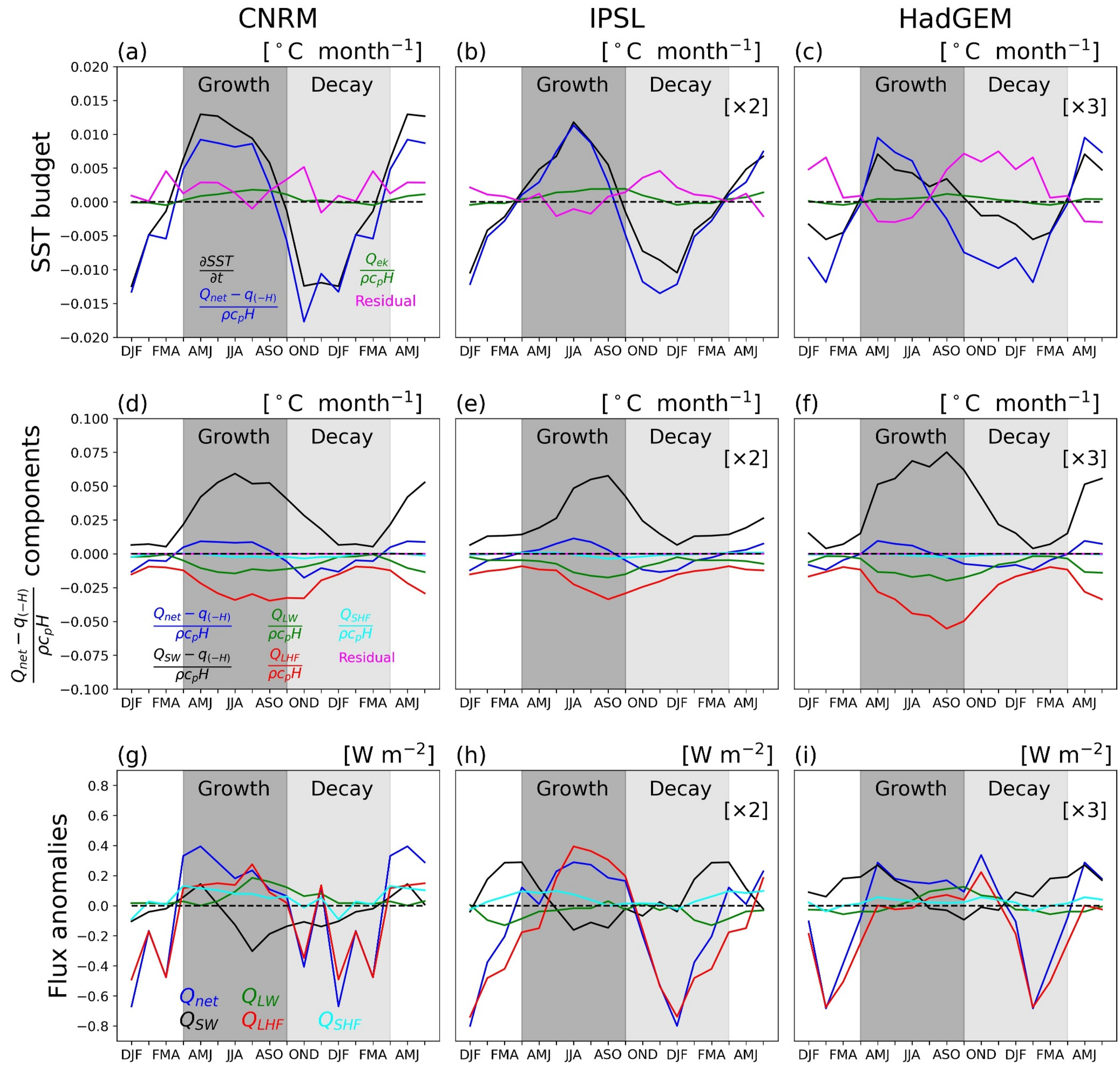

Figure 3. Left panel: (a) SST budget terms (in °C month^{-1}) in Equation 1, (d) components of Q_{net} terms (in °C month^{-1}) in the right-hand side of Equation 1, and (g) Flux anomalies (in W m^{-2}) over tropical North Atlantic Ocean in CNRM model. The middle and right panels are similar to the left panel but for IPSL and HadGEM models. Dark and light gray indicates the growth and decay phases. A 3-month running mean is applied to smooth the time series. Panels in IPSL and HadGEM models are scaled by factors of 2 and 3, as indicated in the panel, to maintain consistent y-axis values for all the plots. A positive value of flux indicates the warming of the ocean.

anomaly and one that depends on the mixed-layer depth anomaly (see Equation 2 in Methods). We first focus on the growth phase, during which the Q_{SW} term plays a dominant role in the SST budget (i.e., Figures 3d–3f). The results from the decomposition are shown in Figure 4.

The anomalous mixed-layer depth term dominates the contribution of the Q_{SW} term to the SST budget in all models (red line; Figures 4a–4c). This indicates that the absorption of climatological Q_{SW} in the tropical North Atlantic acts to enhance the warming of the SST in response to a shallowing of the mixed-layer (solid black line; Figures 4g–4i). In contrast, the direct contribution of the anomalous Q_{SW} has only a small - and opposite - impact

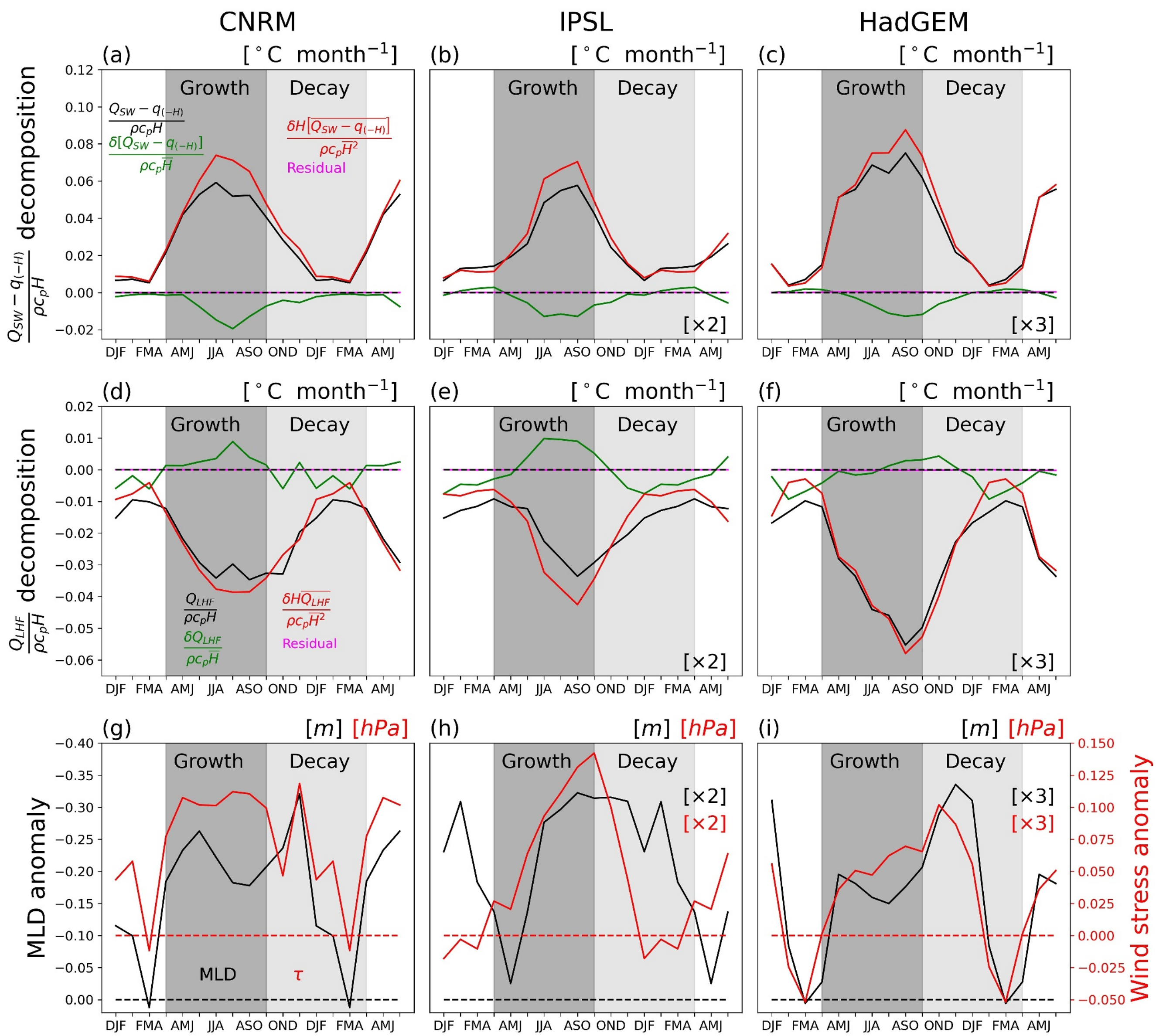

Figure 4. Left panel: Decomposition of (a) Q_{SW} term (in °C month^{-1}) and (d) Q_{LHF} term (in °C month^{-1}) in Equation 2, (g) MLD (solid black line, in m) and horizontal wind stress anomaly (solid red line, in *Pa*) over tropical North Atlantic Ocean in CNRM model. Black and red dotted lines indicate the zero line for MLD and horizontal wind stress anomaly, respectively. The middle and right panels are similar to the left panel but for IPSL and HadGEM models. Dark and light gray indicates the growth and decay phases. A 3-month running mean is applied to smooth the time series. Panels in IPSL and HadGEM models are scaled by factors of 2 and 3, as indicated in the panel, to maintain consistent *y*-axis values for all the plots. A positive value of flux indicates the warming of the ocean.

on the SST tendency (green line; Figures 4a–4c), consistent with the direct cooling effect by the Q_{SW} anomalies seen during the growth phase (in Figures 3g–3i).

The decomposition of the Q_{LHF} budget term is shown in Figures 4d–4f. Again, the anomalous mixed-layer depth term (red line) significantly influences the SST tendency, while the direct impact of the anomalous latent heat-flux (green line) is fairly modest. The cooling by the anomalous mixed-layer depth term represents the release of climatological Q_{LHF} over a shallower mixed-layer, acting to cool SSTs. In other words, latent heat-flux is consistently negative as it releases heat from the ocean through evaporation, cooling the ocean. A shallower mixed-layer depth amplifies this effect, enhancing SST cooling with the same climatological release of latent heat-flux. The effects of both the Q_{SW} and Q_{LHF} terms in the SST budget (Figures 3d–3f) are, therefore, dominated by the effect of a shallower mixed-layer (Figures 4a–4f). Similar results are observed in the decomposition of the

Q_{net}, Q_{LW}, and Q_{SHF} budget terms (Figure S4 in Supporting Information S1). The influence of the Q_{SW} term (black line; Figures 3d–3f) is somewhat offset by the Q_{LHF} term (red line; Figures 3d–3f) during the warm-season growth phase, but the total impact of the Q_{SW} term still dominates the Q_{net} term and is the leading cause of the warming (blue line; Figures 3d–3f).

To summarize, in the experiments with extratropical SST-restoring analyzed here, the warming of the tropical North Atlantic SSTs associated with the positive AMV is caused by the penetration of incoming climatological solar radiation into a shallower mixed-layer. This warming mostly occurs during the extended boreal summer season. Given the dominant role of the mixed-layer in this process, it is important to examine what is causing the shallower mixed-layer during the positive AMV phase.

The evolution of the mixed-layer depth anomaly is shown in Figures 4g–4i (solid black line). During the summer growth phase of tropical AMV, there is clear shoaling throughout the season, with the mixed-layer depth anomaly approaching zero again during the winter season as the climatological mixed-layer deepens (Figure S5 in Supporting Information S1). To examine the source of the mixed-layer depth anomalies, we calculated the wind stress anomalies over the tropical Atlantic region (solid red line, Figures 4g–4i). The variability of the trade winds is related to the cyclonic circulation induced by the warm midlatitude SST anomalies (Figure 1). The shallowing seen during the summer growth phase is associated with a weakening of the northeasterly trade winds (i.e., positive horizontal wind-stress anomalies). In winter, the trade wind anomalies reduce, leading to a reduction in the mixed-layer depth anomalies and the decaying phase of the tropical SST anomalies. The relationship between the trade winds and the mixed-layer depth suggests that it is the trade winds that are controlling the evolution of the mixed-layer depth in the tropical Atlantic and, therefore, the tropical SST evolution.

Whilst the shoaling of the mixed-layer in the summer seems to be driven by changes in the trade winds, the shoaling could be driven by associated changes in surface buoyancy forcing (due to the surface heat-fluxes) or through direct mechanical wind stirring (e.g., Qiu and Kelly (1993)). To explore the relative contributions of each of these, we calculated Monin-Obukhov depth (H_{MO}) anomalies and the contribution of the individual surface buoyancy forcing and mechanical wind stirring terms during the summer season (using Equation 3; see Methods and Table S2 in Supporting Information S1). In the CNRM model, for example, the H_{MO} anomaly ($=-0.39$ m) is primarily driven by the mechanical wind stirring term ($=-0.35$ m), while the surface buoyancy forcing is negligible ($=-0.03$); similar results are found for the IPSL and HadGEM models (Table S2 in Supporting Information S1). The dominance of the mechanical wind stirring found in this calculation is consistent with our analysis above, showing a lack of consistency in the surface heat-flux anomalies (i.e., Figures 2b and 3g–3i). Therefore, we conclude that the anomalies in the mixed-layer depth - which have a dominant impact on tropical SST warming - are primarily caused by anomalies in the mechanical wind stirring associated with the trade wind anomalies.

6. Discussion and Conclusion

In this study, we have examined the evolution of the tropical part of the AMV through extratropical North Atlantic SST-restoring experiments from three climate-coupled models, finding a consistent dynamic evolution of the seasonal SST tendency across the models. Previous studies have proposed wind-evaporation-SST (Chang et al., 1997; Smirnov & Vimont, 2012; Yamamoto et al., 2020; R. Zhang et al., 2019), cloud feedback (Bellomo et al., 2016; Brown et al., 2016; Yuan et al., 2016), and dust feedback (Wang et al., 2012; Yuan et al., 2016) mechanisms, which have all been argued to influence the tropical North Atlantic SST by modulating the net downward surface heat-flux (see Introduction and R. Zhang et al. (2019)). These studies have limitations (see introduction) and have not considered the effect of variable mixed-layer depth, often assuming it to be invariant (e.g., Bellomo et al., 2016; Smirnov & Vimont, 2012). However, when accounting for upper ocean mixed-layer dynamics, we find that changes in surface heat-fluxes or associated mechanisms are not responsible for generating tropical AMV in the experiments analyzed here. Instead, we demonstrate that the development of tropical AMV is dominated by the modulation of mixed-layer depth.

The evolution broadly comprises two phases: initially, the tropical AMV SST anomalies grow from April to October; the SST anomalies then decay from November to March. As the amplitude of the SST tendency in the growth phase surpasses that of the decay phase, the tropical Atlantic warms overall during positive phases of AMV. In the summer months, the trade winds weaken in association with low pressure in the extratropical North

Atlantic region, leading to a shallowing of the mixed-layer. The absorption of the climatological solar radiation being distributed across this shallower mixed-layer acts to increase the SSTs, contributing to positive SST anomalies in the tropical part of the AMV. During the winter months, the trade winds return toward climatological values, and the mixed-layer depth anomalies reduce in magnitude. Simultaneously, the release of climatological latent heat-flux from the shallow mixed-layer dominates, resulting in a damping of SST anomalies in the tropical AMV during winter.

In a previous study, Bellomo et al. (2016) estimated that cloud feedbacks contribute only 10%–17% of observed tropical Atlantic SST anomalies associated with the AMV, but they argued that this may be important in amplifying the tropical AMV signal. In the experiments analyzed in this study, we find the cloud cover anomalies in both the IPSL and HadGEM models during the growth period in our analysis are ≈1%–2% (Figure S6 in Supporting Information S1), which is of similar magnitude to the observed anomalies evaluated by Bellomo et al. (2016). However, in the experiments analyzed here, we have shown that the direct impact of the associated shortwave heat-flux anomalies is negligible. While they may act to amplify the tropical AMV, they do not seem to play a primary role in driving its evolution. In their analysis, Bellomo et al. (2016) did not consider the role of upper ocean dynamics, including mixed-layer depth variability, which here we have found to be crucial.

An important result of our analysis has been the distinct seasonality of the development of the tropical arm of AMV. Whilst the three models analyzed all showed growth during the boreal summer, there are some notable seasonal amplitude differences across the models (Figure 1). It is possible that differences in the mean state of the model, particularly the mean heat-fluxes and/or climatological mixed-layer depth, are contributing to the model differences in annual mean SST amplitude in tropical AMV (Figure S7 in Supporting Information S1). For instance, during DJF, the tropical AMV amplitude in the CNRM model is lower or absent compared to IPSL and HadGEM models (Figure 1). Understanding these differences likely requires a larger multi-model ensemble, but is highlighted here as an important avenue of further investigation given the sensitivity of the atmosphere to tropical SSTs.

Our study demonstrates that, in these SST-restoring experiments, the tropical part of the AMV emerges due to a weakening of the summer trade winds and an associated shallowing of the mixed-layer. The experiments analyzed in this study have proven valuable to constrain the development of tropical AMV in response to extratropical SST anomalies. We did not consider the role of other oceanic contributions, such as horizontal and vertical advection terms, suggesting that ocean dynamics may dampen SST tendencies during the growth and decay phases, particularly offsetting the larger cooling in the decay phase. However, an important focus of future studies will be to analyze whether similar mechanisms are active in the evolution of the observed AMV, including other oceanic terms in the free-running climate model simulations. Tropical AMV anomalies tend to follow the emergence of extratropical AMV anomalies in free-running climate model simulations (e.g., Drews & Greatbatch, 2017; Lai et al., 2022), indicating that the mechanisms analyzed in this study may be responsible. In addition, our study highlights the potential important seasonality in the mechanisms governing the development of the tropical part of AMV, which have not been considered in other studies. Exploring these mechanisms further, including in coupled models and observations, is a priority for future studies on tropical AMV.

Previous studies have emphasized the role of externally forced surface flux changes in driving AMV (Bellomo et al., 2018; Bellucci et al., 2017; Booth et al., 2012; He et al., 2023; Klavans et al., 2022; Murphy et al., 2017, 2021; Otterå et al., 2010; Watanabe & Tatebe, 2019). However, the SST-restoring experiments used here do not incorporate variable external forcing. Therefore, understanding the role of this newly proposed mechanism within free-running models that include variable external forcing is an important avenue for future research on this topic.

Data Availability Statement

The model outputs used in this study are all openly accessible from the CMIP6 archive (https://esgf-index1.ceda.ac.uk/search/cmip6-ceda/) with the following search constraints: "CMIP6" in MIP era, "DCPP" as activity, and two experiment IDs: "dcppC-amv-ExTrop-pos" and "dcppC-amv-ExTrop-neg".

Acknowledgments

We thank the World Climate Research Programme, particularly its Working Group on Coupled Modelling, for coordinating and promoting CMIP6. We are grateful to the modeling groups of component C under the Decadal Climate Prediction Project for their efforts in producing and sharing simulations used in this study. We also thank the Earth System Grid Federation (ESGF) for archiving data and facilitating access, and to the various funding agencies supporting CMIP6 and ESGF initiatives. BS was supported by project funding from the Royal Society. COR was supported by a Royal Society University Research Fellowship. JR was funded by the Natural Environment Research Council (NERC) through the WISHBONE (NE/T013516/1) and CANARI projects (NE/W004984/1).

References

Alexander, M. A., & Scott, J. D. (2008). The role of Ekman ocean heat transport in the northern hemisphere response to ENSO. *Journal of Climate*, *21*(21), 5688–5707. https://doi.org/10.1175/2008jcli2382.1

Bellomo, K., Clement, A. C., Murphy, L. N., Polvani, L. M., & Cane, M. A. (2016). New observational evidence for a positive cloud feedback that amplifies the Atlantic multidecadal oscillation. *Geophysical Research Letters*, *43*(18), 9852–9859. https://doi.org/10.1002/2016gl069961

Bellomo, K., Murphy, L. N., Cane, M. A., Clement, A. C., & Polvani, L. M. (2018). Historical forcings as main drivers of the Atlantic multidecadal variability in the CESM large ensemble. *Climate Dynamics*, *50*(9–10), 3687–3698. https://doi.org/10.1007/s00382-017-3834-3

Bellucci, A., Mariotti, A., & Gualdi, S. (2017). The role of forcings in the twentieth-century north Atlantic multidecadal variability: The 1940–75 north Atlantic cooling case study. *Journal of Climate*, *30*(18), 7317–7337. https://doi.org/10.1175/jcli-d-16-0301.1

Boer, G. J., Smith, D. M., Cassou, C., Doblas-Reyes, F., Danabasoglu, G., Kirtman, B., et al. (2016). The decadal climate prediction project (DCPP) contribution to CMIP6. *Geoscientific Model Development*, *9*(10), 3751–3777. https://doi.org/10.5194/gmd-9-3751-2016

Booth, B. B., Dunstone, N. J., Halloran, P. R., Andrews, T., & Bellouin, N. (2012). Aerosols implicated as a prime driver of twentieth-century north Atlantic climate variability. *Nature*, *484*(7393), 228–232. https://doi.org/10.1038/nature10946

Brown, P. T., Lozier, M. S., Zhang, R., & Li, W. (2016). The necessity of cloud feedback for a basin-scale Atlantic multidecadal oscillation. *Geophysical Research Letters*, *43*(8), 3955–3963. https://doi.org/10.1002/2016gl068303

Chang, P., Ji, L., & Li, H. (1997). A decadal climate variation in the tropical Atlantic ocean from thermodynamic air-sea interactions. *Nature*, *385*(6616), 516–518. https://doi.org/10.1038/385516a0

Davis, R., DeSzoeke, R., & Niiler, P. (1981). Variability in the upper ocean during mile. Part II: Modeling the mixed layer response. *Deep-Sea Research, Part A: Oceanographic Research Papers*, *28*(12), 1453–1475. https://doi.org/10.1016/0198-0149(81)90092-3

Delworth, T. L., & Mann, M. E. (2000). Observed and simulated multidecadal variability in the northern hemisphere. *Climate Dynamics*, *16*(9), 661–676. https://doi.org/10.1007/s003820000075

Deser, C., Alexander, M. A., Xie, S.-P., & Phillips, A. S. (2010). Sea surface temperature variability: Patterns and mechanisms. *Annual Review of Marine Science*, *2*(1), 115–143. https://doi.org/10.1146/annurev-marine-120408-151453

Dong, B., Sutton, R. T., & Scaife, A. A. (2006). Multidecadal modulation of El Niño–Southern Oscillation (ENSO) variance by Atlantic Ocean sea surface temperatures. *Geophysical Research Letters*, *33*(8), L08705. https://doi.org/10.1029/2006gl025766

Drews, A., & Greatbatch, R. J. (2017). Evolution of the Atlantic multidecadal variability in a model with an improved north Atlantic current. *Journal of Climate*, *30*(14), 5491–5512. https://doi.org/10.1175/jcli-d-16-0790.1

Frankignoul, C. (1985). Sea surface temperature anomalies, planetary waves, and air-sea feedback in the middle latitudes. *Reviews of Geophysics*, *23*(4), 357–390. https://doi.org/10.1029/rg023i004p00357

Goldenberg, S. B., Landsea, C. W., Mestas-Nuñez, A. M., & Gray, W. M. (2001). The recent increase in Atlantic hurricane activity: Causes and implications. *Science*, *293*(5529), 474–479. https://doi.org/10.1126/science.1060040

He, C., Clement, A. C., Kramer, S. M., Cane, M. A., Klavans, J. M., Fenske, T. M., & Murphy, L. N. (2023). Tropical Atlantic multidecadal variability is dominated by external forcing. *Nature*, *622*(7983), 521–527. https://doi.org/10.1038/s41586-023-06489-4

Hodson, D. L., Robson, J. I., & Sutton, R. T. (2014). An anatomy of the cooling of the North Atlantic Ocean in the 1960s and 1970s. *Journal of Climate*, *27*(21), 8229–8243. https://doi.org/10.1175/jcli-d-14-00301.1

Kavvada, A., Ruiz-Barradas, A., & Nigam, S. (2013). AMO'S structure and climate footprint in observations and IPCC AR5 climate simulations. *Climate Dynamics*, *41*(5–6), 1345–1364. https://doi.org/10.1007/s00382-013-1712-1

Kerr, R. A. (2000). A north Atlantic climate pacemaker for the centuries. *Science*, *288*(5473), 1984–1985. https://doi.org/10.1126/science.288.5473.1984

Klavans, J. M., Clement, A. C., Cane, M. A., & Murphy, L. N. (2022). The evolving role of external forcing in north Atlantic SST variability over the last millennium. *Journal of Climate*, *35*(9), 2741–2754. https://doi.org/10.1175/jcli-d-21-0338.1

Knight, J. R., Folland, C. K., & Scaife, A. A. (2006). Climate impacts of the Atlantic multidecadal oscillation. *Geophysical Research Letters*, *33*(17), L17706. https://doi.org/10.1029/2006gl026242

Kraus, E., & Turner, J. (1967). A one-dimensional model of the seasonal thermocline ii. the general theory and its consequences. *Tellus*, *19*(1), 98–106. https://doi.org/10.3402/tellusa.v19i1.9753

Kucharski, F., Ikram, F., Molteni, F., Farneti, R., Kang, I.-S., No, H.-H., et al. (2016). Atlantic forcing of pacific decadal variability. *Climate Dynamics*, *46*(7–8), 2337–2351. https://doi.org/10.1007/s00382-015-2705-z

Lai, W., Robson, J., Wilcox, L., & Dunstone, N. (2022). Mechanisms of internal atlantic multidecadal variability in HADGEM3-GC3. 1 at two different resolutions. *Journal of Climate*, *35*(4), 1365–1383. https://doi.org/10.1175/jcli-d-21-0281.1

Liu, G., Kwon, Y.-O., Frankignoul, C., & Lu, J. (2023). Understanding the drivers of Atlantic multidecadal variability using a stochastic model hierarchy. *Journal of Climate*, *36*(4), 1043–1058. https://doi.org/10.1175/jcli-d-22-0309.1

Martin, E. R., Thorncroft, C., & Booth, B. B. (2014). The multidecadal Atlantic SST—Sahel rainfall teleconnection in CMIP5 simulations. *Journal of Climate*, *27*(2), 784–806. https://doi.org/10.1175/jcli-d-13-00242.1

McGregor, S., Timmermann, A., Stuecker, M. F., England, M. H., Merrifield, M., Jin, F.-F., & Chikamoto, Y. (2014). Recent walker circulation strengthening and pacific cooling amplified by atlantic warming. *Nature Climate Change*, *4*(10), 888–892. https://doi.org/10.1038/nclimate2330

Monerie, P.-A., Robson, J., Dong, B., Hodson, D. L., & Klingaman, N. P. (2019). Effect of the Atlantic multidecadal variability on the global monsoon. *Geophysical Research Letters*, *46*(3), 1765–1775. https://doi.org/10.1029/2018gl080903

Morioka, Y., Tozuka, T., Masson, S., Terray, P., Luo, J.-J., & Yamagata, T. (2012). Subtropical dipole modes simulated in a coupled general circulation model. *Journal of Climate*, *25*(12), 4029–4047. https://doi.org/10.1175/jcli-d-11-00396.1

Morioka, Y., Tozuka, T., & Yamagata, T. (2010). Climate variability in the southern Indian Ocean as revealed by self-organizing maps. *Climate Dynamics*, *35*(6), 1059–1072. https://doi.org/10.1007/s00382-010-0843-x

Morioka, Y., Tozuka, T., & Yamagata, T. (2011). On the growth and decay of the subtropical dipole mode in the south Atlantic. *Journal of Climate*, *24*(21), 5538–5554. https://doi.org/10.1175/2011jcli4010.1

Murphy, L. N., Bellomo, K., Cane, M., & Clement, A. (2017). The role of historical forcings in simulating the observed Atlantic multidecadal oscillation. *Geophysical Research Letters*, *44*(5), 2472–2480. https://doi.org/10.1002/2016gl071337

Murphy, L. N., Klavans, J. M., Clement, A. C., & Cane, M. A. (2021). Investigating the roles of external forcing and ocean circulation on the Atlantic multidecadal SST variability in a large ensemble climate model hierarchy. *Journal of Climate*, *34*(12), 4835–4849. https://doi.org/10.1175/jcli-d-20-0167.1

O'Reilly, C. H., Patterson, M., Robson, J., Monerie, P. A., Hodson, D., & Ruprich-Robert, Y. (2023). Challenges with interpreting the impact of Atlantic multidecadal variability using SST-restoring experiments. *npj Climate and Atmospheric Science*, *6*(1), 14. https://doi.org/10.1038/s41612-023-00335-0

O'Reilly, C. H., Woollings, T., & Zanna, L. (2017). The dynamical influence of the Atlantic multidecadal oscillation on continental climate. *Journal of Climate*, *30*(18), 7213–7230. https://doi.org/10.1175/jcli-d-16-0345.1

Otterå, O. H., Bentsen, M., Drange, H., & Suo, L. (2010). External forcing as a metronome for Atlantic multidecadal variability. *Nature Geoscience*, *3*(10), 688–694. https://doi.org/10.1038/ngeo955

Paulson, C. A., & Simpson, J. J. (1977). Irradiance measurements in the upper ocean. *Journal of Physical Oceanography*, *7*(6), 952–956. https://doi.org/10.1175/1520-0485(1977)007<0952:imituo>2.0.co;2

Qiu, B., & Kelly, K. A. (1993). Upper-ocean heat balance in the Kuroshio extension region. *Journal of Physical Oceanography*, *23*(9), 2027–2041. https://doi.org/10.1175/1520-0485(1993)023<2027:uohbit>2.0.co;2

Ruprich-Robert, Y., Delworth, T., Msadek, R., Castruccio, F., Yeager, S., & Danabasoglu, G. (2018). Impacts of the Atlantic multidecadal variability on north American summer climate and heat waves. *Journal of Climate*, *31*(9), 3679–3700. https://doi.org/10.1175/jcli-d-17-0270.1

Ruprich-Robert, Y., Msadek, R., Castruccio, F., Yeager, S., Delworth, T., & Danabasoglu, G. (2017). Assessing the climate impacts of the observed Atlantic multidecadal variability using the GFDL CM2. 1 and NCAR CESM1 global coupled models. *Journal of Climate*, *30*(8), 2785–2810. https://doi.org/10.1175/jcli-d-16-0127.1

Senapati, B., Morioka, Y., Behera, S. K., & Dash, M. K. (2024). Southern hemisphere circumpolar wavenumber-4 pattern simulated in SINTEX-F2 coupled model. *Journal of Geophysical Research: Oceans*, *129*(7), e2023JC020801. https://doi.org/10.1029/2023jc020801

Smirnov, D., & Vimont, D. J. (2012). Extratropical forcing of tropical Atlantic variability during boreal summer and fall. *Journal of Climate*, *25*(6), 2056–2076. https://doi.org/10.1175/jcli-d-11-00104.1

Sutton, R. T., & Hodson, D. L. (2005). Atlantic Ocean forcing of North American and European summer climate. *Science*, *309*(5731), 115–118. https://doi.org/10.1126/science.1109496

Sutton, R. T., & Hodson, D. L. (2007). Climate response to basin-scale warming and cooling of the North Atlantic Ocean. *Journal of Climate*, *20*(5), 891–907. https://doi.org/10.1175/jcli4038.1

Ting, M., Kushnir, Y., Seager, R., & Li, C. (2011). Robust features of Atlantic multi-decadal variability and its climate impacts. *Geophysical Research Letters*, *38*(17), L17705. https://doi.org/10.1029/2011gl048712

Wang, C., Dong, S., Evan, A. T., Foltz, G. R., & Lee, S.-K. (2012). Multidecadal covariability of North Atlantic Sea surface temperature, African dust, Sahel rainfall, and Atlantic hurricanes. *Journal of Climate*, *25*(15), 5404–5415. https://doi.org/10.1175/jcli-d-11-00413.1

Watanabe, M., & Tatebe, H. (2019). Reconciling roles of sulphate aerosol forcing and internal variability in Atlantic multidecadal climate changes. *Climate Dynamics*, *53*(7), 4651–4665. https://doi.org/10.1007/s00382-019-04811-3

Yamamoto, A., Tatebe, H., & Nonaka, M. (2020). On the emergence of the Atlantic multidecadal SST signal: A key role of the mixed layer depth variability driven by North Atlantic Oscillation. *Journal of Climate*, *33*(9), 3511–3531. https://doi.org/10.1175/jcli-d-19-0283.1

Yuan, T., Oreopoulos, L., Zelinka, M., Yu, H., Norris, J. R., Chin, M., et al. (2016). Positive low cloud and dust feedbacks amplify tropical north Atlantic multidecadal oscillation. *Geophysical Research Letters*, *43*(3), 1349–1356. https://doi.org/10.1002/2016gl067679

Zhang, L., & Wang, C. (2013). Multidecadal north Atlantic Sea surface temperature and Atlantic meridional overturning circulation variability in CMIP5 historical simulations. *Journal of Geophysical Research: Oceans*, *118*(10), 5772–5791. https://doi.org/10.1002/jgrc.20390

Zhang, R., & Delworth, T. L. (2006). Impact of Atlantic multidecadal oscillations on India/SAHEL rainfall and Atlantic hurricanes. *Geophysical Research Letters*, *33*(17), L17712. https://doi.org/10.1029/2006gl026267

Zhang, R., Sutton, R., Danabasoglu, G., Kwon, Y.-O., Marsh, R., Yeager, S. G., et al. (2019). A review of the role of the Atlantic meridional overturning circulation in Atlantic multidecadal variability and associated climate impacts. *Reviews of Geophysics*, *57*(2), 316–375. https://doi.org/10.1029/2019rg000644